Magnon damping by magnon-phonon coupling in manganese perovskites

Pengcheng Dai
Oak Ridge National Laboratory, Oak Ridge, Tennessee 37831-6393

H. Y. Hwang
Bell Laboratories, Lucent Technologies, Murray Hill, New Jersey 07974

Jiandi Zhang
Department of Physics, Florida International University, University Park, Miami, Florida 33199

J. A. Fernandez-Baca
Oak Ridge Natinal Laboratory, Oak Ridge, Tennessee 37831-6393

S.-W. Cheong
Bell Laboratories, Lucent Technologies, Murray Hill, New Jersey 07974
and Department of Physics and Astronomy, Rutgers University, Piscataway, New Jersey 08855

C. Kloc
Bell Laboratories, Lucent Technologies, Murray Hill, New Jersey 07974

Y. Tomioka
Joint Research Center for Atom Technology (JRCAT), Tsukuba 305 8562, Japan

Y. Tokura
Joint Research Center for Atom Technology (JRCAT), Tsukuba 305 8562, Japan
and Department of Applied Physics, University of Tokyo, Tokyo 113 8656, Japan
(Received 27 October 1999)

Inelastic neutron scattering was used to systematically investigate the spin-wave excitations (magnons) in ferromagnetic manganese perovskites. In spite of the large differences in the Curie temperatures (T_C's) of different manganites, their low-temperature spin waves have very similar dispersions with the zone-boundary magnon softening and broadening that cannot be explained by the canonical double exchange mechanism. From the wave-vector dependence of the magnon lifetime effects and its correlation with the dispersions of the optical-phonon modes, we argue that a strong magnetoelastic (magnon-phonon) coupling is responsible for the observed low-temperature anomalous spin dynamical behavior of the manganites.

The elementary magnetic excitations (spin waves or magnons) in a ferromagnet can provide direct information about the itinerancy of the unpaired electrons contributing to the ordered moment. In insulating (local moment) ferromagnets, such excitations are usually well defined throughout the Brillouin zone and can be described by the Heisenberg model of magnetism.[1] On the other hand, metallic (itinerant) ferromagnets are generally characterized by the disappearance of spin waves at finite energy and momentum due to the presence of the Stoner (electron-hole pair) excitation continuum associated with the band structure and itinerant electrons in the system.[2] In the mixed valent ferromagnetic manganese perovskites (manganites) $A_{0.7}B_{0.3}MnO_3$ (where A and B are rare-earth and alkaline-earth elements, respectively),[3] the ferromagnetism and zero-temperature electric conductivity can be continually suppressed by different $A(B)$ substitutions until an insulating, charge-ordered ground state is stabilized.[4] Due to the octahedral crystalline field, the $3d$ energy levels of the Mn^{3+} ion in $A_{0.7}B_{0.3}MnO_3$ split into a lower t_{2g} triplet, forming an $S=3/2$ core spin, and an upper e_g doublet, the conduction band. For manganites with higher Curie temperature (T_C) and lower residual resistivity, the low-temperature spin-wave excitations are that of a conventional metallic ferromagnet and their dispersions can be described by a simple Heisenberg Hamiltonian with the nearest-neighbor exchange coupling.[5–7] Indeed, such behavior is expected from the canonical double exchange (DE) mechanism[8] in the strong-coupling limit, where the hopping kinetic energy (t) of the conduction band (e_g) electrons is much less than the intra-atomic (Hund-rule coupling) exchange energy J_H ($J_H/t\rightarrow\infty$).[9–11] With decreasing T_C and increasing residual resistivity, anomalous softening and broadening of magnons deviating from the simple Heisenberg Hamiltonian were observed near zone boundary at low temperatures.[12] The question is whether such anomaly is purely electronic in origin[13,14] or the consequence of electron-lattice coupling known to be important to the transport properties of these materials around T_C.[15,16] In particular, if DE mechanism alone is insufficient and electron-lattice coupling must be included to explain the anomalous behav-

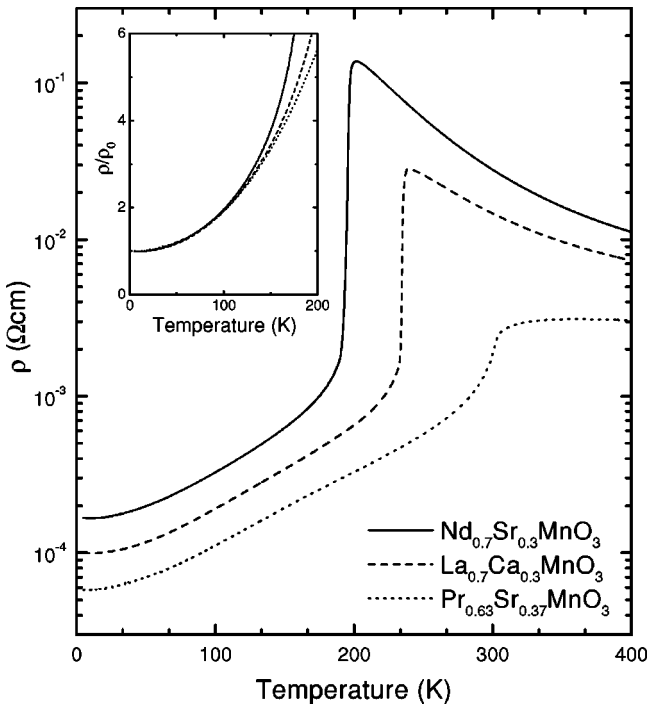

FIG. 1. Temperature dependence of the resistivity $\rho(T)$ for single crystals used in the neutron-scattering experiments. The large drop in $\rho(T)$ corresponds to the Curie temperature (T_C) of our samples. They are 301, 238, and 198 K for PSMO, LCMO, and NSMO, respectively. The inset shows the normalized resistivity $\rho(T)/\rho(0)$, it is clear that all three samples have the same $\rho(T)/\rho(0)$ temperature dependence below about 100 K.

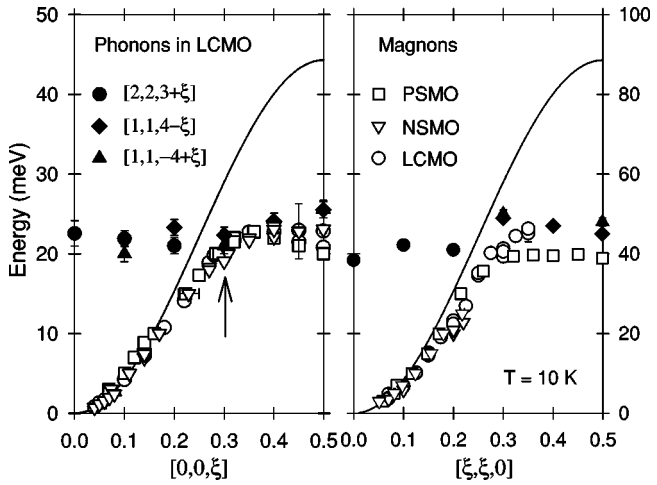

FIG. 2. Open symbols show magnon dispersions along the $[0,0,\xi]$ and $[\xi,\xi,0]$ directions for ~30% manganites PSMO (open squares), LCMO (open circles), and NSMO (open down triangles) at 10 K. The data for PSMO are from Ref. 13. The solid line is a fit to a nearest-neighbor Hamiltonian assuming isotropic spin waves for $\xi<0.1$. Full symbols show selected LO phonon modes collected along the reciprocal-lattice directions as specified in the legend. The rapid decrease of the manganese magnetic form factor at these large wave vectors ensure that the scattering stem mostly from the lattice vibrations (phonons).

ior, it is important to establish how electrons couple to the underlying lattice on a microscopic scale.[17,18]

Here we present inelastic neutron-scattering data that suggest a microscopic origin for the observed low-temperature spin-wave softening and broadening. By comparing spin-wave excitations of three manganite single crystals that have approximately the same nominal carrier concentration but significantly different T_C's and residual resistivity (see Fig. 1), we show that the single-band DE model and Heisenberg Hamiltonian do not capture the physics of their spin dynamical properties. Moreover, from the wave-vector dependence of the magnon lifetime effects and its association with the dispersions of selected optical phonon modes, we argue that the observed magnon softening and broadening are due to strong magnetoelastic (or magnon-phonon) interactions, consistent with the electron-lattice coupling for the manganites in the proximity of the charge ordered insulating state.

For this study, we prepared ferromagnetic pseudocubic single crystals of $Pr_{0.63}Sr_{0.37}MnO_3$ (PSMO), $La_{0.7}Ca_{0.3}MnO_3$ (LCMO), and $Nd_{0.7}Sr_{0.3}MnO_3$ (NSMO) by floating zone technique. The properties of PSMO and NSMO were decribed in detail previously.[19] The LCMO single crystal is approximately 0.4 cm^3 in volume and has mosaic of about 1°. The experiments were performed using the HB-1, HB-2, and HB-3 triple-axis spectrometers at the High-Flux Isotope reactor of the Oak Ridge National Laboratory. Most of the spin-wave measurements were carried out on the HB-1 spectrometer with pyrolytic graphite as the monochromator, analyzer, and filters. The final neutron energy was fixed at E_f =13.6 meV with typical collimations of, proceeding from the reactor to the detector, 48-40-60-120 min (full width at half maximum). To label wave vectors in reciprocal space, we use reciprocal-lattice units (rlu) such that the momentum transfer (q_x,q_y,q_z) in units of $Å^{-1}$ are at reciprocal space positions $(H,K,L)=(q_xa/2\pi,q_ya/2\pi,q_za/2\pi)$ rlu, where a (≈3.86 Å) is the lattice parameter of the pseudocubic unit cell. In this notation, the zone boundary along the $[0,0,\xi]$ direction for ferromagnetic spin waves is at the (0,0,0.5) rlu. For the experiment, we oriented the crystals such that wave vectors in the form of (H,H,L) rlu can be accessed in the horizontal scattering plane.

The temperature-dependent resistivity $\rho(T)$ for these three samples is shown in Fig. 1. The characteristic drop in ρ coincident with T_C is clearly seen to increase with decreasing T_C. At the same time the residual resistivity increases almost linearly with decreasing T_C, indicating that the system becomes a worse metal at low temperatures for materials with larger magnetoresistance effect. An interesting feature of $\rho(T)$ at low temperatures is that all three samples exhibit the same temperature dependence below ~100 K when $\rho(T)$ is scaled to the residual value $\rho(0)$. The inset to Fig. 1 illustrates this point.

The open symbols in Fig. 2 summarize the spin-wave dispersions along two high symmetry directions at 10 K for PSMO, LCMO, and NSMO. Clearly, the dispersions of these three manganites are remarkably similar at the measured frequencies, indicating that the magnetic exchange coupling strength, derived from the hopping of the e_g electrons between the Mn^{3+} and Mn^{4+} sites, depend only weakly on T_C. These results are in sharp contrast to the single-band DE model where the spin-wave dispersions are directly related to electronic bandwidth and hence T_C.[9–11] In the strong-

coupling limit of this model, the spin-wave dispersion of the ferromagnet is consistent with the nearest-neighbor Heisenberg Hamiltonian and the spin-wave stiffness constant D should be proportional to the electron transfer energy t. Previous work has shown that such single-band DE model is adequate for describing the spin dynamics of the highest T_C ferromagnetic manganites.[5–7] To estimate the spin-spin exchange coupling strength, we note that the low-frequency spin waves of $A_{0.7}B_{0.3}MnO_3$ manganites LCMO,[20] NSMO, and PSMO (Ref. 19) are isotropic and gapless with a stiffness $D \approx 165$ meV Å^{-2}. For a simple cubic Heisenberg ferromagnet with nearest-neighbor exchange coupling J, $D = 2JSa^2$, where S is the magnitude of the electronic spin at the magnetic ionic sites and a ($a \simeq 3.86$ Å) is the lattice parameter. From the measured spin-wave stiffness, one can calculate the exchange coupling strength J and hence the expected dispersion for a simple nearest-neighbor Heisenberg ferromagnet. The solid lines in Fig. 2 show the outcome of such calculation which clearly misses the measured spin-wave energies at large wave vectors.

Figure 3 shows typical constant-**q** scans along the $[0,0,\xi]$ and $[\xi,\xi,0]$ directions for LCMO and NSMO. Most of the data are well described by Gaussian fits which give the amplitude, widths, and peak positions of the excitations. While the dispersion curves shown in Fig. 2 are obtained by peak positions at different wave vectors, the amplitude and widths provide information about the damping and lifetime of the magnon excitations. Figure 3(a) displays the result along the $[0,0,\xi]$ direction and similar data along the $[\xi,\xi,0]$ direction is shown in Fig. 3(b). It is clear that spin waves are significantly damped at large wave vectors. Although still relatively well defined throughout the Brillouin zone in the $[0,0,\xi]$ direction for both compounds, the excitations are below the sensitivity of the measurements at wave vectors beyond (0.25,0.25,0) rlu along the $[\xi,\xi,0]$ direction for NSMO.

To further investigate the wave-vector dependence of the spin-wave broadening and damping, we plot in Fig. 4 the intrinsic widths of the magnons along the $[0,0,\xi]$ direction. The full width at half maximum (FHWM) of the excitations Γ shows a similar increase at wave vectors larger than $\xi \approx 0.3$ rlu for all three manganites. To determine whether such broadening is due to the Stoner continuum, we note that at low temperatures, the spin moment of itinerant electrons of ferromagnetic manganites is completely saturated and the system is in the half-metallic state.[21] In this scenario of the DE model, there is complete separation of the majority and minority band by a large J_H. As a consequence, the Stoner continuum is expected to lie at an energy scale ($2J_H$) much higher than that of the spin-wave excitations.[10] For this reason, the observed magnon broadening and damping for lower T_C manganites are unlikely to be due to Stoner continuum excitations.[22]

On the other hand, such behavior may be well understood if one assumes a different spin-wave damping channel that is related to a strong coupling between the conduction band (e_g) electrons and the cooperative oxygens in the Mn-O-Mn bond, analogous to that of a dynamic Jahn-Teller (JT) effect.[17] Although JT based electron-lattice coupling is known to be important for the metal-to-insulator transition at

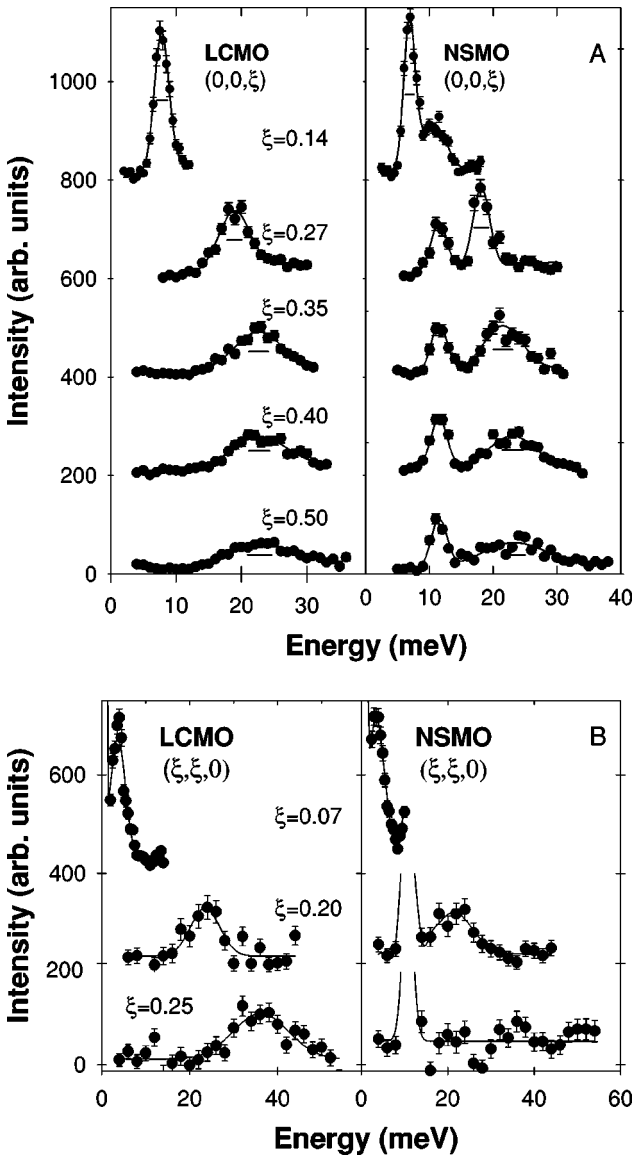

FIG. 3. Constant-**q** scans at selected wave vectors for LCMO and NSMO at 10 K along the $[0,0,\xi]$ (**A**) and $[\xi,\xi,0]$ (**B**) directions. The data were taken with PG as monochromator and analyzer at a final neutron energy of $E_f = 13.6$ meV. Analyzer turned background have been subtracted from the data. The magnetic nature of the signal was confirmed by measuring the temperature and wave-vector dependence of the scattering (see Fig. 2 of Ref. 13). There is a dispersionless crystal electric-field (CEF) level at ~12 meV from Nd for NSMO. The horizontal bars show the resolution along the scan direction. Solid lines are Gaussian fits to the data.

temperatures near and above T_C,[15,16] such coupling may also be important to understand the low-temperature magnetic properties.

If electron-lattice coupling is indeed responsible for the observed spin-wave broadening and damping, one would expect the presence of such coupling in the lower T_C samples that should be absent in the higher T_C materials. Experimentally, there have been no reports of magnon-phonon coupling in the higher T_C $A_{0.7}B_{0.3}MnO_3$.[5,6] For the DE ferromagnet $La_{0.8}Sr_{0.2}MnO_3$ ($T_C = 304$ K), Moudden *et al.*[7] have measured the spin-wave, acoustic, and optical-phonon disper-

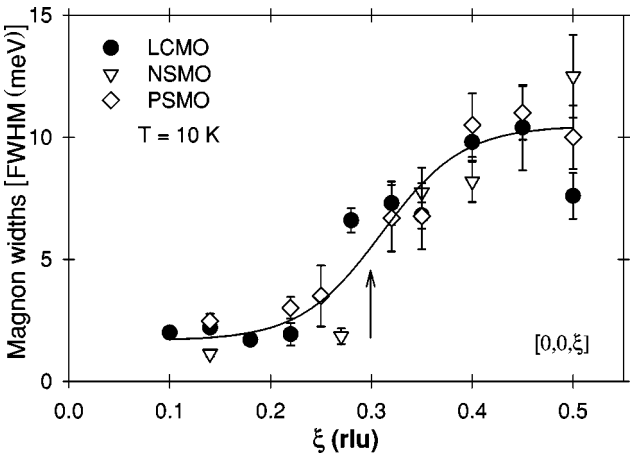

FIG. 4. The intrinsic magnon widths Γ along the $[0,0,1+\xi]$ direction for PSMO, LCMO, and NSMO at 10 K. To obtain Γ, we have deconveluted the spin-wave widths from the instrumental resolution calculated using the spin-wave dispersion at the measured wave vectors. Significant broadening of Γ is seen at $\xi \approx 0.3$ rlu. The arrow indicates the crossing point of magnon and phonon dispersions. Solid line is the guide to the eye.

sions from the zone center to the zone boundary along the $[0,0,\xi]$ direction. Phonon branches were found to cross smoothly through the magnon dispersion with no hint of magnon-phonon hybridization. Similar results were found in $La_{0.75}Ca_{0.25}MnO_3$.[23] For ferromagnet $La_{0.7}Ca_{0.3}MnO_3$, infrared reflectivity spectra show three zone center ($\mathbf{q}=0$) transverse-optical (TO) phonons located around 20.4, 42, and 73 meV.[24] These three phonon modes were identified as ''external,'' ''bending,'' and ''stretching'' modes which correspond to the vibration of the La/Ca ions against the MnO_6 octahedron, the bending motion of the Mn-O-Mn bond, and the internal motion of the Mn ion against the oxygen octahedron, respectively.

To search for possible magnon-phonon coupling in the lower T_C manganites, we have measured selected optical phonons in the LCMO single crystal. Figure 2 shows two longitudinal optical (LO) phonon modes throughout the Brillouin zone as solid symbols. The energies of the two LO modes observed by neutron scattering at $\mathbf{q}=0$ are very close to that the external and bending modes identified by infrared reflectivity.[24] At wave vectors larger than 0.3 rlu, the dispersions of these two phonon modes are remarkably close to those of the magnons along the $[0,0,\xi]$ and $[\xi,\xi,0]$ directions. This suggest that the softening of the spin-wave branches in Fig. 2 may be due to the magnon-phonon coupling.

In principle, the interaction between the magnetic moments and the lattice can modify spin waves in two different ways. First, the static lattice deformation induced by the ordered magnetic moments may affect the anisotropy of the spin waves. Second, the dynamic time-dependent modulations of the magnetic moment may interfere with the lattice vibrations, resulting in significant magnetoelastic interactions or magnon-phonon coupling. One possible consequence of such coupling is to create energy gaps in the magnon dispersion at the nominal intersections of the magnon and phonon modes. Our spin-wave dispersion data in Fig. 2 show no obvious evidence for such gap at the magnon and phonon crossing at $\xi \approx 0.3$ rlu. However, we cannot rule out the presence of such gap because the broad nature of the scattering for $\xi > 0.3$ [Fig. 3(a)]. Alternatively, magnon-phonon coupling, present in all exchange coupled magnetic compounds to some extent, may give rise to spin-wave broadening.[25] In this scenario, the vibrations of the magnetic ions about their equilibrium positions affect the exchange energy through the spatial variation of the spin-spin exchange coupling strength, which in turn leads to spin-wave broadening at the magnon-phonon crossing points. Generally, one would expect such coupling to be strong for the lower T_C $A_{0.7}B_{0.3}MnO_3$ manganites because of their close proximity to the charge-ordered insulating state.[4] This is exactly what is observed for these materials at $\xi \geqslant 0.3$ rlu along the $[0,0,\xi]$ direction. Constant-$\mathbf{q}$ scans [Fig. 3(a)] show sudden broadening of the spin waves from wave vector $\xi = 0.27$ to 0.35 rlu in LCMO and NSMO. Similarly, Fig. 4 reveals that magnon widths increase considerably at wave vectors $\xi \geqslant 0.3$ rlu for all three manganites investigated, consistent with the expectation of a strong magnon-phonon hybridization.

We have discovered that spin-wave softening and broadening along the $[0,0,\xi]$ direction occur at the nominal intersection of the magnon and optical phonon modes in lower T_C $A_{0.7}B_{0.3}MnO_3$ manganites. This result strongly suggests that magnetoelastic coupling is important to the understanding of the low-temperature spin dynamics of $A_{0.7}B_{0.3}MnO_3$. In the lower doping canted ferromagnet $La_{0.85}Sr_{0.15}MnO_3$,[26] much larger spin-wave broadening and damping were found at low temperatures.[27] Although the magnon dispersion relation in that system appears to be consistent with the simple nearest-neighbor Heisenberg Hamiltonian, the observation of strong anisotropic spin-wave broadening is in sharp contrast to the expectation of the single-band DE model where magnons in the ground state are eigenstates of the system.[27] Therefore it becomes clear that the single-band DE mechanism cannot describe the spin dynamics of $La_{0.85}Sr_{0.15}MnO_3$ and lower T_C $A_{0.7}B_{0.3}MnO_3$ manganites, not even in the low-temperature ground state. To understand the extraordinary magnetic and transport properties of $A_{1-x}B_xMnO_3$, one must explicitly consider the close coupling between charge, spin, and lattice degrees of freedom in these complex materials.

We thank H. Kawano, N. Furukawa, S. W. Lovesey, W. E. Plummer, S. E. Nagler, H. G. Smith, and X. D. Wang for helpful discussions. This work was supported by the US DOE under Contract No. DE-AC05-96OR22464 with Lockheed Martin Energy Research Corporation and JRCAT of Japan.

[1] W. Heisenberg, Z. Phys. **49**, 619 (1928).
[2] T. Izuyama *et al.*, J. Phys. Soc. Jpn. **18**, 1025 (1963).
[3] G. H. Jonker and J. H. Van Santen, Physica (Amsterdam) **16**, 337 (1950).
[4] H. Y. Hwang, S.-W. Cheong, P. G. Radaelli, M. Marezio, and B. Batlogg, Phys. Rev. Lett. **75**, 914 (1995).
[5] M. C. Martin, G. Shirane, Y. Endoh, K. Hirota, Y. Moritomo, and Y. Tokura, Phys. Rev. B **53**, 14 285 (1996).
[6] T. G. Perring, G. Aeppli, S. M. Hayden, S. A. Carter, J. P. Remeika, and S.-W. Cheong, Phys. Rev. Lett. **77**, 711 (1996).
[7] A. H. Moudden, L. Visiliu-Doloc, L. Pinsard, and A. Revcolevschi, Physica B **241**, 276 (1998).
[8] C. Zener, Phys. Rev. **82**, 403 (1951).
[9] K. Kubo and N. Ohata, J. Phys. Soc. Jpn. **33**, 21 (1972).
[10] N. Furukawa, J. Phys. Soc. Jpn. **65**, 1174 (1996).
[11] T. A. Kaplan and S. D. Mahanti, J. Phys.: Condens. Matter **9**, L291 (1997).
[12] H. Y. Hwang, P. Dai, S.-W. Cheong, G. Aeppli, D. A. Tennant, and H. A. Mook, Phys. Rev. Lett. **80**, 1316 (1998).
[13] X. D. Wang, Phys. Rev. B **57**, 7427 (1998).
[14] I. V. Solovyev and K. Terakura, Phys. Rev. Lett. **82**, 2959 (1999).
[15] A. J. Millis, B. I. Shraiman, and R. Mueller, Phys. Rev. Lett. **77**, 175 (1996).
[16] H. Röder, J. Zang, and A. R. Bishop, Phys. Rev. Lett. **76**, 1356 (1996).
[17] J.-S. Zhou and J. B. Goodenough, Phys. Rev. Lett. **80**, 2665 (1998).
[18] G. Khaliullin and R. Kilian, Phys. Rev. B **61**, 3494 (2000).
[19] J. A. Fernandez-Baca, P. Dai, H. Y. Hwang, C. Kloc, and S.-W. Cheong, Phys. Rev. Lett. **80**, 4012 (1998).
[20] J. W. Lynn, R. W. Erwin, J. A. Borchers, Q. Huang, A. Santoro, J. L. Peng, and Z. Y. Li, Phys. Rev. Lett. **76**, 4046 (1996).
[21] J.-H. Park, E. Vescovo, H. J. Kim, C. Kwon, R. Ramesh, and T. Venkatesan, Nature (London) **392**, 794 (1998).
[22] Reference 13 suggests that the observed broadening in PSMO at low temperature is due to the disappearance of spin waves into the Stoner continuum in the intermediate coupling regime of the single-band DE model. However, remarkable similarities in magnon dispersions and broadening (Figs. 2–4) seen for samples with widely different T_C's argue against this possibility. In the single-band model, T_C is expected to be directly related magnon dispersions, bandwidths, and hence Stoner continuum.
[23] P. Dai *et al.* (unpublished).
[24] K. H. Kim, J. Y. Gu, H. S. Choi, G. W. Park, and T. W. Noh, Phys. Rev. Lett. **77**, 1877 (1996).
[25] S. W. Lovesey, *Theory of Neutron Scattering from Condensed Matter* (Clarendon Press, Oxford, 1984), Vol. 2, p. 126.
[26] H. Kawano, R. Kajimoto, M. Kubota, and H. Yoshizawa, Phys. Rev. B **53**, 2202 (1996).
[27] L. Vasiliu-Doloc, J. W. Lynn, A. H. Moudden, A. M. de Leon-Guevara, and A. Revcolevschi, Phys. Rev. B **58**, 14 913 (1998).